Propagation of acoustic waves in nematic elastomers

E. M. Terentjev,[1] I. V. Kamotski,[2] D. D. Zakharov,[2] and L. J. Fradkin[2]
[1]*Cavendish Laboratory, University of Cambridge, Cambridge CB3 0HE, United Kingdom*
[2]*School of Engineering, South Bank University, London SE1 0AA, United Kingdom*
(Received 26 February 2002; published 20 November 2002)

We develop a theory of elastic waves in oriented monodomain nematic elastomers. The effect of soft elasticity, combined with the Leslie-Ericksen version of dissipation function, results in an unusual dispersion and anomalous anisotropy of shear acoustic waves. A characteristic time scale of nematic rotation determines the crossover frequency, below which waves of some polarizations have a very strong attenuation while others experience no dissipation at all. We study the anisotropy of low-frequency Poynting vectors and wave fronts, and discuss a ''squeeze'' effect of energy transfer nonparallel to the wave vector. Based on these theoretical results, an application, the acoustic polarizer, is proposed.

DOI: 10.1103/PhysRevE.66.052701 PACS number(s): 83.80.Va, 61.41.+e, 62.30.+d

Liquid crystalline elastomers (LCE) represent an exciting physical system that combines the local orientational symmetry breaking and the entropic rubber elasticity, producing a number of unique physical phenomena. In ordinary elastic solids, the deformations are created by relative movement of the same atoms (or molecules) that form the bonded low-symmetry lattice. Hence, when the deformation is small, the lattice symmetry is preserved and one obtains an ordinary anisotropic elastic response. In contrast, in polymer networks, the macroscopic elasticity arises from the entropy change of chains on relative movement of their cross-linked end points, which are relatively far apart. On a smaller length scale, a liquid crystalline order can be established within these chains. In nematic elastomers, the local director can rotate, in principle, independently of deformation of the cross-linking points. Such an internal degree of freedom within the elastic body constitutes what is known as the Cosserat medium: the relative movement of cross-linking points provides elastic strains and forces, while the director rotation causes local torques and couple stresses. Recent review articles summarize these ideas and report physical effects, predicted theoretically and found experimentally in nematic LCE; e.g., Refs. [1,2].

A pioneering study of oscillating dynamic-mechanical properties [3] has been followed by further work on aligned monodomain nematic LCE, [4,5], which demonstrated a dramatic reduction of storage elastic modulus G' and the associated increase in the loss factor $\tan\delta$ in certain geometries of deformation. This effect, named the ''dynamic soft elasticity,'' allows one to directly probe the basic equilibrium properties of nematic rubbers and also access the new kinetic parameters—viscous coefficients and relaxation times.

Here we follow the earlier theoretical work [6], which formulated the constitutive relations of linear viscoelasticity for nematic elastomers in the hydrodynamic (low-frequency) limit, and develop a theory of acoustic waves propagating through an elastic medium with the mobile anisotropic microstructure and dissipation. Viscoelastic waves in anisotropic media have been thoroughly investigated over the last decade [7]. We apply a similar analysis to the nematic rubbers and obtain unusual predictions for directions of energy propagation and conditions for anomalous dissipation. We also find the configurations of propagation and polarization, where the attenuation vanishes. This ''acoustic polarization,'' similar to the optical polarization in a birefringent medium, could lead to many new discoveries and applications.

Equilibrium elastic properties of monodomain nematic rubbers are well studied, both theoretically and experimentally, and are described at some length in review articles. A molecular theory of ideal nematic networks [8] gives the elastic free energy density in terms of the Cauchy strain tensor and the the uniaxial matrices of chain step lengths before and after the director $\boldsymbol{n}$ has rotated by a certain angle during the deformation: $\ell_{ij}=\ell_\perp\delta_{ij}+[\ell_\parallel-\ell_\perp]n_in_j$. One finds that, apart from the universal rubber-elastic energy scale $\mu=c_xk_BT$, with c_x proportional to the cross-linking density, the theory depends on a single equilibrium parameter $r=\ell_\parallel/\ell_\perp$, the ratio of the principal step lengths of the anisotropic polymer backbone [or equivalently, $r=(R_\parallel/R_\perp)^2$ for the principal values of gyration radii]. This ratio is a function of the nematic order parameter.

As in all polymeric materials, the bulk modulus is independent of the configurational entropy of polymer chains and mainly determined by molecular forces resisting the compression of a liquid, $\tilde{B}\sim10^{10}$ J/m^3, much greater than the typical value of rubber modulus $\mu\sim10^6$ J/m^3. In this paper, we shall explicitly implement the incompressible limit.

The small-deformation limit of the elastic energy depends on $\tilde{\varepsilon}_{ik}=\varepsilon_{ik}-\frac{1}{3}\mathrm{Tr}[\underline{\underline{\boldsymbol{\varepsilon}}}]\delta_{ik}$, the traceless part of linear symmetric strain $\varepsilon_{ik}=\frac{1}{2}(\partial_ku_i+\partial_iu_k)$, with $\boldsymbol{u}$ the displacement vector, which is the only variable of classical continuum elasticity [9]. In a system with an internal orientational degree of freedom, the antisymmetric part of strain, $\boldsymbol{\Omega}=\frac{1}{2}\mathrm{curl}\,\boldsymbol{u}$, also contributes to the physical response via the relative rotation, denoted here by the vector $\boldsymbol{\Theta}\equiv\boldsymbol{\Omega}-[\boldsymbol{n}\times\delta\boldsymbol{n}]$. The elastic potential energy density of a uniaxial incompressible solid takes the form [10]

$$F=C_1(\boldsymbol{n}\cdot\underline{\underline{\boldsymbol{\varepsilon}}}\cdot\boldsymbol{n})^2+2C_4[\boldsymbol{n}\times\underline{\underline{\boldsymbol{\varepsilon}}}\times\boldsymbol{n}]^2+4C_5([\boldsymbol{n}\times\underline{\underline{\boldsymbol{\varepsilon}}}\cdot\boldsymbol{n}])^2+\frac{1}{2}D_1[\boldsymbol{n}\times\boldsymbol{\Theta}]^2+D_2\boldsymbol{n}\cdot\underline{\underline{\boldsymbol{\varepsilon}}}\cdot[\boldsymbol{n}\times\boldsymbol{\Theta}]. \quad (1)$$

All constants in Eq. (1) are of the same order of magnitude,

similar to the rubber modulus μ, and can be explicitly represented as functions of r [8]. In the isotropic phase, the elastic energy reduces to the classical Lamé expression.

The Leslie-Ericksen theory of anisotropic viscous dissipation in a nematic liquid can be written using the same symmetry grouping of terms as in Eq. (1) [6]. The entropy production density is a quadratic form of the corresponding velocities:

$$T\dot{s}=A_1(\boldsymbol{n}\cdot\dot{\underline{\boldsymbol{\varepsilon}}}\cdot\boldsymbol{n})^2+2A_4[\boldsymbol{n}\times\dot{\underline{\boldsymbol{\varepsilon}}}\times\boldsymbol{n}]^2+4A_5([\boldsymbol{n}\times\dot{\underline{\boldsymbol{\varepsilon}}}\cdot\boldsymbol{n}])^2 + \frac{1}{2}\gamma_1[\boldsymbol{n}\times\dot{\boldsymbol{\Theta}}]^2+\gamma_2\boldsymbol{n}\cdot\dot{\underline{\boldsymbol{\varepsilon}}}\cdot[\boldsymbol{n}\times\dot{\boldsymbol{\Theta}}]. \tag{2}$$

It describes two types of dissipations, by shear flow and by rotation of the director, and vanishes for rigid rotations. The constants are linear combinations of classical Leslie coefficients. In the isotropic limit, one finds a single shear viscosity, $A_1=2A_4=2A_5\rightarrow\eta$. The identical symmetry of variables and their velocities leads to the viscous coefficients represented as products of the corresponding elastic constants and appropriate relaxation times:

$$A_i\approx\tau_R C_i,\quad \gamma_1\approx\tau_1 D_1,\quad \gamma_2\approx\tau_2 D_2, \tag{3}$$

where τ_R is of the order of Rouse time for the corresponding polymer backbone, while $\tau_{1,2}$ are the nematic relaxation times. One expects, in many polymer systems, to find $\tau_R\sim10^{-5}$–10^{-6} s [11], while the nematic director relaxation time is $\tau_1\sim10^{-2}$ s from Ref. [12].

Since the elastic potential energy has a similar form as the entropy production, the equations of motion for both the translational and the rotational degrees of freedom are similar to the classical Leslie-Ericksen theory [6,13]:

$$\rho\ddot{\boldsymbol{u}}=\nabla\cdot\underline{\boldsymbol{\sigma}}^{\mathrm{sym}}, \tag{4}$$

$$0=\boldsymbol{n}\times[(D_1+\gamma_1\partial_t)[\boldsymbol{n}\times\boldsymbol{\Theta}]+(D_2+\gamma_1\partial_t)\boldsymbol{n}\cdot\underline{\boldsymbol{\varepsilon}}], \tag{5}$$

where the second equation is the balance of torques. Choosing the coordinate axis $\boldsymbol{e}_3$ along the undistorted director $\boldsymbol{n}$, the components of the symmetric part of the stress tensor take the form

$$\begin{aligned}
\sigma_{11}^{\mathrm{sym}}&=4(C_4+A_4\partial_t)\varepsilon_{11},\\
\sigma_{22}^{\mathrm{sym}}&=4(C_4+A_4\partial_t)\varepsilon_{22},\\
\sigma_{33}^{\mathrm{sym}}&=2(C_1+A_1\partial_t)\varepsilon_{33},\\
\sigma_{13}^{\mathrm{sym}}&=4(C_5+A_5\partial_t)\varepsilon_{13}-\tfrac{1}{2}(D_2+\gamma_2\partial_t)\Theta_2,\\
\sigma_{23}^{\mathrm{sym}}&=4(C_5+A_5\partial_t)\varepsilon_{23}+\tfrac{1}{2}(D_2+\gamma_2\partial_t)\Theta_1,\\
\sigma_{12}^{\mathrm{sym}}&=4(C_4+A_4\partial_t)\varepsilon_{12}.
\end{aligned} \tag{6}$$

Since we are only interested in small distortions of the material, the convective contribution to all material derivatives are neglected.

Let us seek the elastic wave solutions of our dissipative dynamic system in the usual form

$$\boldsymbol{u}(t,\boldsymbol{x})=\boldsymbol{U}e^{i\omega t-i\boldsymbol{k}\cdot\boldsymbol{x}}, \tag{7}$$

where $\boldsymbol{U}=(U_1,U_2,U_3)$ is the amplitude vector. In order to obtain a closed equation for the elastic displacement $\boldsymbol{u}(t,\boldsymbol{x})$, we need to eliminate the rotational variable $\boldsymbol{\Theta}$ from the stress in the right hand side of Eq. (4). This is a straightforward procedure of substituting the formal solution of Eq. (5),

$$\begin{pmatrix}\Theta_1\\ \Theta_2\end{pmatrix}=\frac{D_2+i\omega\gamma_2}{D_1+i\omega\gamma_1}\begin{pmatrix}-\varepsilon_{23}\\ \varepsilon_{13}\end{pmatrix}, \tag{8}$$

into the corresponding components of stress $\underline{\boldsymbol{\sigma}}^{\mathrm{sym}}$. This operation [6,14,15] is known as the integration out of the internal degree of freedom. In the absence of viscous terms, the result is the famous renormalization of the shear modulus C_5, leading to the soft-elasticity condition. In our case, it is complicated by the viscous terms, but the essence remains the same,

$$C_5^R(\omega)=C_5-\frac{D_2^2}{8D_1}\frac{(1+i\omega\tau_2)^2}{(1+i\omega\tau_R)(1+i\omega\tau_1)} \tag{9}$$

[neglecting the small differences between relaxation times $\tau_R(i)$ for each C_i-A_i pair]. Another aspect of this renormalization is a constraint on relaxation times. It is easy to check that the stability requirement of non-negativity of the average $T\dot{s}$ demands $A_5-\gamma_2^2/8\gamma_1\geqslant0$, which in turn, requires that $\tau_1\tau_R\geqslant\tau_2^2$ in ideally soft materials.

Substituting Eq. (7) into the resulting renormalized version of Eq. (4), we arrive at the set of algebraic equations for the unknown amplitude vector, wave vector, and frequency, $\boldsymbol{U}$, $\boldsymbol{k}$ and ω:

$$[(1+i\omega\tau_R)\underline{\boldsymbol{\Lambda}}(\omega,k)-\rho\omega^2\underline{\mathbb{I}}]\boldsymbol{U}=0, \tag{10}$$

where $\underline{\mathbb{I}}$ is the 3×3 unit matrix and $\underline{\boldsymbol{\Lambda}}$ is the symmetric matrix with elements,

$$\begin{aligned}
\Lambda(\omega,\boldsymbol{k})_{11}&=4C_4k_1^2+2C_4k_2^2+2C_5^R(\omega)k_3^2,\\
\Lambda(\omega,\boldsymbol{k})_{22}&=2C_4k_1^2+4C_4k_2^2+2C_5^R(\omega)k_3^2,\\
\Lambda(\omega,\boldsymbol{k})_{33}&=2C_5^R(\omega)(k_1^2+k_2^2)+2C_1k_3^2,\\
\Lambda(\omega,\boldsymbol{k})_{12}&=2C_4k_1k_2,\\
\Lambda(\omega,\boldsymbol{k})_{13}&=2C_5^R(\omega)k_1k_3,\\
\Lambda(\omega,\boldsymbol{k})_{23}&=2C_5^R(\omega)k_2k_3.
\end{aligned} \tag{11}$$

The matrix $\underline{\boldsymbol{\Lambda}}$ has the same structure as arises in the theory of the wave propagation in classical, uniaxially symmetric (transversely isotropic) solids [16]; the crucial difference for nematic elastomers is the frequency-dependent renormalized constant $C_5^R(\omega)$.

In general, the anisotropic medium supports three different complex speeds of wave propagation $c=\omega/k$, which de-

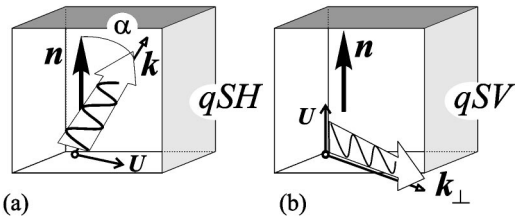

FIG. 1. Diagram of wave propagation for (a) qSH wave, with $\boldsymbol{U}^{\mathrm{qSH}} \| \boldsymbol{n} \times \hat{\boldsymbol{k}}$, and (b) qSV wave, with $\boldsymbol{U}^{\mathrm{qSV}} \| \boldsymbol{n}$.

termine uniquely the kinematic and dynamical properties of the corresponding waves. We concentrate here on the so-called homogeneous plane waves when the wave vector may be written as $\boldsymbol{k} \equiv (\mathrm{Re}\, k + i\, \mathrm{Im}\, k)\hat{\boldsymbol{k}}$, with the real unit vector $\hat{\boldsymbol{k}}$ specifying the unique direction, and $\mathrm{Re}\, k$ and $\mathrm{Im}\, k$ having different signs [18]. Traditionally, the principal types of waves, as determined by their speeds, are called quasicompressional (qP), quasishear horizontal (qSH), and quasishear vertical (qSV) [17]. It is possible to show that the quasicompressional waves do not satisfy the incompressibility condition and, therefore, are not considered in this paper. The quasishear waves have the respective vector amplitudes: $\boldsymbol{U}^{\mathrm{qSH}} \| \boldsymbol{n} \times \hat{\boldsymbol{k}}$, for $\hat{\boldsymbol{k}} \| \boldsymbol{n}$, see Fig. 1(a), and a complicated form of $\boldsymbol{U}^{\mathrm{qSV}}$ is given, e.g., by Eq. (3.12) in Ref. [17]. The special case of $\hat{\boldsymbol{k}} \| \boldsymbol{n}$ is mentioned below.

It follows that the wave amplitudes depend on the angle α between $\hat{\boldsymbol{k}}$ and $\boldsymbol{n}$. The dispersion relationships are easily obtained from the general Eq. (10). For the qSH waves, we have

$$\rho\omega^2 = 2[C_4(k_1^2 + k_2^2) + C_5^R(\omega)k_3^2](1 + i\omega\tau_{\mathrm{R}}), \qquad (12)$$

$$c_{\mathrm{qSH}}^2 = \frac{2}{\rho}[C_4 \sin^2\alpha + C_5^R(\omega)\cos^2\alpha](1 + i\omega\tau_{\mathrm{R}}), \qquad (13)$$

the last equation describing the square of the complex speed $c_{\mathrm{qSH}}(\omega, \alpha)$.

In general, the qSV waves are not purely shear and thus, not always satisfy the incompressibility condition. However, when the wave vectors $\boldsymbol{k} = \boldsymbol{k}_\perp$ lie in the plane of isotropy perpendicular to $\boldsymbol{n}$, they can carry the qSV waves, which are purely shear for all frequencies, with their amplitude vectors $\boldsymbol{U}_\parallel$ in the direction of $\boldsymbol{n}$, see Fig. 1(b). The corresponding dispersion relationship and the resulting complex speed are

$$\rho\omega^2 = 2C_5^R(\omega)(1 + i\omega\tau_{\mathrm{R}})k_\perp^2, \qquad (14)$$

$$c_{\mathrm{qSV}}^2 = \frac{2}{\rho}C_5^R(\omega)(1 + i\omega\tau_{\mathrm{R}}). \qquad (15)$$

Finally, we remark that when $\hat{\boldsymbol{k}} \| \boldsymbol{n}$, the corresponding amplitude vector $\boldsymbol{U}_\perp$ is arbitrary in the plane of isotropy. In this case, the qSV speed equals the qSH speed as given by Eq. (13) at $\alpha = 0$, and therefore, it makes no sense to distinguish between qSV and qSH waves for this geometry.

The corresponding phase velocities $(\mathrm{Re}\, c)\hat{\boldsymbol{k}}$ and attenuations $(-\mathrm{Im}\, k)\hat{\boldsymbol{k}}$ are presented in Fig. 2 for qSH waves, at

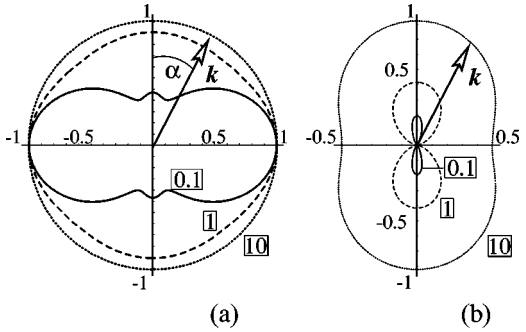

FIG. 2. Polar plots of (a) phase speed $\mathrm{Re}\, c(\omega, \alpha)$, in units of $\sqrt{\mu/\rho}$, and (b) attenuation $\mathrm{Im}\, k(\omega, \alpha)$, in units of $\sqrt{\rho/\mu\tau_1^2}$, for the qSH waves propagating in the meridional plane (the director $\boldsymbol{n}$ is vertical). Curves for $\omega\tau_1 = 0.1$, 1, and 10 are labeled on plots.

dimensionless frequencies $\omega\tau_1 = 0.1$, 1, and 10. In making the plots, we take the typical values of nematic elastomer parameters: $r = 3$ and the Rouse time scale $\tau_{\mathrm{R}} \sim 10^{-2}\tau_1$, following [6,12]. Figure 2 indicates that higher frequencies propagate at a higher speed, but also encounter higher attenuation. However, the low-frequency qSH waves propagating in the plane of isotropy encounter a very small loss; no dissipation at all in the case of the ideally soft nematic elastomer. At $\omega\tau_1 \gg 1$, the director relaxation is frozen and we find the increasing attenuation in all directions.

To study the energy transfer by acoustic waves, let us introduce the mean Poynting vector (the vector of power flow density, averaged over the oscillation period) as $\boldsymbol{P} = -\frac{1}{2}\,\mathrm{Re}\langle \underline{\underline{\boldsymbol{\sigma}}}^{\mathrm{sym}} \cdot \dot{\boldsymbol{u}}^* \rangle$. Figure 3(a) shows the polar plots of the projection $(\boldsymbol{P} \cdot \hat{\boldsymbol{k}})\hat{\boldsymbol{k}}$ and the complementary projection $\boldsymbol{P} \cdot (\underline{\underline{\mathbb{I}}} - \hat{\boldsymbol{k}}\hat{\boldsymbol{k}})$, for $\omega\tau_1 = 0.1$ and 1, in units of $\mu^{3/2}\rho^{-1/2}$. Note that for $\omega\tau_1 \ll 1$, the energy flows in the direction different to the direction of wave propagation, and it turns out that (unless both lie in the equatorial plane of isotropy or along $\boldsymbol{n}$) the wave vector $\hat{\boldsymbol{k}}$ is always closer to the $\boldsymbol{n}$ axis than the Poynting vector. At $\omega\tau_1 \gg 1$, we find $\hat{\boldsymbol{k}}$ is approximately $\| \boldsymbol{P}$.

In Fig. 3(b), we present the wave front, which is defined following Ref. [7] as the locus of the end points of the energy velocity vectors,

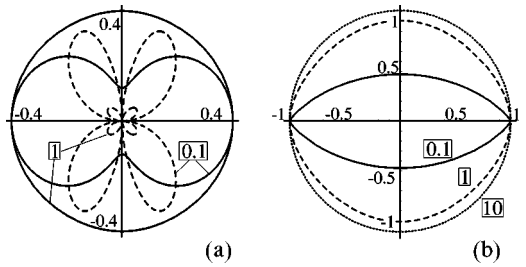

FIG. 3. Polar plots, in the meridional plane around $\boldsymbol{n}$, of (a) the projection of the Poynting vector on $\hat{\boldsymbol{k}}$ (solid lines) and the complementary projection (dashed lines), and (b) the wave front for the qSH waves, for $\omega\tau_1 = 0.1$, 1, and 10. The amplitude of $\boldsymbol{P}$ increases with frequency and, at $\omega\tau_1 = 0.1$, P is scaled up by a factor of 100, to fit on the same graph.

$$c_E = \frac{2P}{\langle \frac{1}{2}\rho \dot{\boldsymbol{u}}\cdot\dot{\boldsymbol{u}}^* + \frac{1}{2}\mathrm{Re}\,\underline{\underline{\boldsymbol{\sigma}}}^{sym}:\underline{\underline{\boldsymbol{\varepsilon}}}^* \rangle},$$

where in denominator, one finds the total mean energy density: the sum of the kinetic and the real part of the complex strain energy density; the latter can be conveniently evaluated as $(1/2)\rho\omega^2 \exp[2i\arg(c)]\boldsymbol{u}\cdot\boldsymbol{u}^*$ for homogeneous waves.

Figures 2 and 3 show that attenuation and energy transfer functions are much more anisotropic than the solid itself. In particular, in the plane isotropy ($\alpha=\pi/2$), no attenuation takes place for the qSH waves; the phase speed is $c_{\mathrm{qSH}} \approx \sqrt{2C_4/\rho}$. Figure 3(b) shows that under the above conditions, the energy velocity is at its maximum and is also frequency independent.

Nonideal (semisoft) nematic elastomers have a small correction to the principal relative-rotation constant D_1 [6,8], deflecting it from an exact ''soft-elasticity'' condition $C_5 - D_1^2/8D_2 = 0$; all other coefficients could remain the same as in the ideal case. A large body of experimental evidence suggests that the semisoft correction, $D_1 \to D_1 + a\mu$, is indeed small ($a \ll 1$) in most studied materials. In our case, the results summarized in the figures are modified only slightly. To illustrate, in Fig. 4, we compare the limiting case of (semisoft) qSH wave, propagating in the equatorial plane of isotropy, with the qSV wave. One can see that, for the chosen values of parameters, the qSH phase speed remains constant, while the qSV speed grows with frequency. The low-frequency limit has a singularity in both the qSV speed and its attenuation: $\mathrm{Re}\,c_{\mathrm{qSV}} \approx 2\sqrt{\mu/\rho}(\omega\tau_1)^{1/2}$, before reaching the saturation at $\omega\tau_1 > 1$. (In the semisoft case, the singularity is removed, the speed reaching a small constant value $\mathrm{Re}\,c_{\mathrm{qSV}} \approx 4\sqrt{a\mu/\rho}$. Remarkably, the attenuation of the qSV wave is hundreds of times higher than that of the semisoft qSH($\alpha=\pi/2$) wave; this is the effect of acoustic polarization.

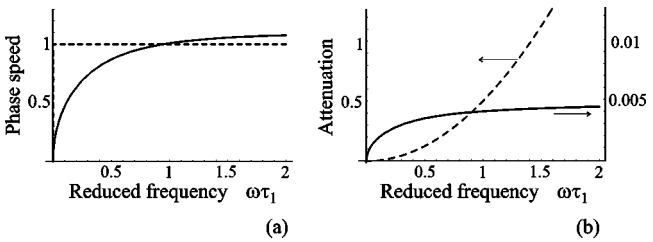

FIG. 4. Comparison between the qSV wave (solid lines) and the case of qSH wave propagating in the plane $\perp \boldsymbol{n}$ (dashed lines): (a) the phase speed and (b) the attenuation; units same as in Fig. 2. Note, that the attenuation for qSH wave at $\alpha=\pi/2$ is very low even for semisoft elastomer and it is scaled up by a factor of 100 to fit on the same graph.

To summarize, we have developed a first-approximation theory of acoustic waves in nematic elastomers: a uniaxial viscoelastic medium with a mobile rotational internal degree of freedom. Results and predictions include the very strong anisotropy of wave attenuation and elastic energy transfer, and theoretical constraints on the possible propagation geometry and material parameters. A possibility of practical application of such materials as efficient acoustic polarizers is very attractive: one only has to look at the effect, the ability to control and manipulate, the optical polarization had on a variety of modern technologies. However, much remains to be investigated in this field. In particular, one needs to reexamine the condition of incompressibility, which we assumed here for simplicity of argument: at higher frequencies, the effect of compressional waves could become noticeable.

We appreciate valuable discussions with M. Warner, T. C. Lubensky, and W. Stille. This work has been supported by the EPSRC, Grant No. GR/M31552, in the Center for Waves and Fields at the School of Engineering of South Bank University.

[1] H. R. Brand and H. Finkelmann, in *Handbook of Liquid Crystals*, edited by D. Demus *et al.* (Wiley-VCH, New York, 1998).
[2] E. M. Terentjev, J. Phys.: Condens. Matter **11**, R239 (1999).
[3] J. L. Gallani, L. Hilliou, P. Martinoty, F. Doublet, and M. Mauzac, J. Phys. II **6**, 443 (1996).
[4] S. M. Clarke, A. R. Tajbakhsh, E. M. Terentjev, and M. Warner, Phys. Rev. Lett. **86**, 4044 (2001).
[5] P. Stein, N. Assfalg, H. Finkelmann, and P. Martinoty, Eur. Phys. J. E **4**, 255 (2001).
[6] E. M. Terentjev and M. Warner, Eur. Phys. J. E **4**, 343 (2001).
[7] J. M. Carcione, Geophysics **60**, 537 (1994).
[8] M. Warner and E. M. Terentjev, Prog. Polym. Sci. **21**, 853 (1996).
[9] L. D. Landau and E. M. Lifshitz, *Theory of Elasticity*, 3rd ed. (Pergamon, Oxford, 1986).
[10] P. G. de Gennes, in *Liquid Crystals of One- and Two-Dimensional Order*, edited by W. Helfrich and G. Heppke (Springer, Berlin, 1980).
[11] M. Doi and S. F. Edwards, *Theory of Polymer Dynamics* (Clarendon, Oxford, 1986).
[12] M. Schonstein, W. Stille, and G. Strobl, Eur. Phys. J. E **5**, 511 (2001).
[13] P. G. de Gennes and J. Prost, *Physics of Liquid Crystals* (Clarendon, Oxford, 1993).
[14] L. Golubovic and T. C. Lubensky, Phys. Rev. Lett. **63**, 1082 (1989).
[15] P. D. Olmsted, J. Phys. II **4**, 2215 (1994).
[16] R. G. Payton, *Elastic Wave Propagation in Transversly Isotropic Media* (Martinus Nijhoff, The Hague, 1983).
[17] P. Chadwick, Proc. R. Soc. London, Ser. A **422**, 23 (1989).
[18] Waves are called inhomogeneous in more exotic situations, when $\mathrm{Im}\,k$ has the same sign as $\mathrm{Re}\,k$ or is zero, or else, when no unique direction can be found for the complex wave vector $\boldsymbol{k}$.